Available online at www.sciencedirect.com
SCIENCE DIRECT®
Journal of Crystal Growth ▮ (▮▮▮▮) ▮▮▮–▮▮▮
JOURNAL OF CRYSTAL GROWTH
www.elsevier.com/locate/jcrysgro

Defect characteristics of ZnO film grown on (0 0 0 1) sapphire with an ultrathin gallium wetting layer

Y. Wang[a,*], X.L. Du[a], Z.X. Mei[a], Z.Q. Zeng[a], Q.Y. Xu[a], Q.K. Xue[a], Z. Zhang[b]

[a]*Beijing National Laboratory for Condensed Matter Physics, Institute of Physics, Chinese Academy of Sciences, Beijing 100080, China*
[b]*Beijing University of Technology, 100 Pingle Yuan, Chao Yang District, Beijing 100022, China*

Received 6 April 2004; accepted 23 August 2004
Communicated by J.B. Mullin

Abstract

The defect characteristics of ZnO film grown on (0 0 0 1) sapphire substrate using an ultrathin Ga wetting layer are investigated by transmission electron microscopy and X-ray diffractometry compared to that of the ZnO film without Ga. It was found that the defects of the ZnO film with a Ga layer were prominently reduced and a high-quality film was formed. Within this ZnO film, most defects near the interface are mixed-type dislocations that interact strongly, leading to a remarkable reduction of dislocations in the upper part of the epitaxial film with a total dislocation density of as low as $8 \times 10^8\,cm^{-2}$. Almost no pure screw dislocations were observed. Furthermore, the film exhibits a single domain structure, and no inversed domains were found. The role of the ultrathin gallium layer in the defect reduction and inversion domain suppression is discussed.

PACS: 68.37.Lp; 81.05.Dz; 61.10.Kw; 68.55.Ln

Keywords: A1. Defects; A1. Diffusion; A1. X-ray diffraction; A3. Molecular beam epitaxy; B1. Zinc compounds

1. Introduction

Recently, wurtzite ZnO and related alloys have attracted great attentions because of their applications in short wavelength light-emitting diodes and diode lasers [1,2]. For these applications, a high-quality single crystalline ZnO film is essential since defects such as threading dislocations (TDs) can act as carrier trap and recombination centers deteriorating the device performance [3]. For example, diodes containing elementary screw dislocations exhibit high prebreakdown reverse leakage currents [4]. ZnO films directly grown on (0 0 0 1) sapphire, however, usually contain a large

*Corresponding author. Beijing Laboratory of Electron Microscopy, Institute of Physics, Chinese Academy of Sciences, P.O. Box 603, Beijing 100080, China. Tel.: 86-10-82648011; fax: 86-10-62561422.
E-mail address: ywang@blem.ac.cn (Y. Wang).

0022-0248/$ - see front matter © 2004 Elsevier B.V. All rights reserved.
doi:10.1016/j.jcrysgro.2004.08.022

number of defects due to the big lattice mismatch (18.4%) between ZnO film and sapphire [5]. The majority of the defects are TDs, their density can be as high as $1.9 \times 10^{11}\,cm^{-2}$ [2]. These defects form at the interface and penetrate into the whole films [6,7]. Meanwhile, inversion domains were also observed in the ZnO epilayers [8]. In order to reduce the defect density, an GaN or MgO interlayer has been used [9,10] to decrease the lattice mismatch. Very recently, a surface modification technique of sapphire substrate using an ultrathin Ga wetting layer has been developed to obtain high-quality ZnO film, and a dramatic defect reduction is achieved [11,12]. In this study, the defect nature in the ZnO film prepared by this method is investigated by transmission electron microscopy (TEM) and X-ray diffractometry (XRD) compared to the ZnO film without the Ga wetting layer, aims to characterize the role of the Ga layer in the defect reduction and inversion domain suppression.

2. Experimental procedure

The samples for this study were grown on sapphire (0 0 0 1) substrate by radio frequency (RF) plasma-assisted molecular beam epitaxy (MBE-IV, ShengYang KeYi). Zinc and gallium were supplied by evaporating 6 N elemental Zn and 6 N elemental Ga from commercial Knudsen cells, respectively. Active oxygen radicals were produced by RF-plasma system (HD25R, Oxford Applied Research). The base pressure in the growth chamber was $\sim 1.210^{-7}$ Pa.

After being degreased in trichloroethylene and acetone, the sapphire substrates were chemically etched for 30 min in a hot solution of H_2SO_4:H_3PO_4 = 3:1 at 140 °C to etched in a hot solution of H_2SO_4:H_3PO_4 = 3:1 at 140 °C for 30 min to remove the surface contamination and the damaged surface layer that was caused by mechanical polishing.

Two samples with different sapphire pretreatment processes were prepared. Sample A was grown directly on the sapphire without any intentional pretreatment. A two-step growth method was employed, i.e., high-temperature epilayer growth at 650 °C after low-temperature buffer layer growth at 400 °C. For sample B, the substrate was thermally cleaned at 750 °C for 30 min and then exposed to the oxygen radicals for 30 min at 400 °C with an RF power of 300 W and oxygen pressure of 1.0×10^{-2} Pa. After the oxygen plasma pretreatment, we switched off the plasma source and evacuated the chamber rapidly down to $\sim 110^{-6}$ Pa. Then, the Ga cell shutter was opened and the Ga deposition started. The deposition rate was about 0.2 Å /s at 820 °C and 22 s later the deposition was finished. The same two-step growth method was adopted as sample A. A high-resolution X-ray diffractometer (Philips) was used to characterize the crystalline of the ZnO epilayers and investigate the in-plane epitaxial relationship between ZnO and sapphire (0 0 0 1).

The TEM experiments were carried out using a Philips CM12 TEM at 100 kV.The cross-sectional specimens were prepared by the conventional method including cutting, gluing, mechanical polishing and dimpling procedures, followed by an Ar+ ion-beam milling for perforation.

3. Results and discussion

Figs. 1(a) and (b) show the cross-sectional TEM (XTEM) images of a ZnO/sapphire film without Ga wetting layer (sample A) under weak-beam

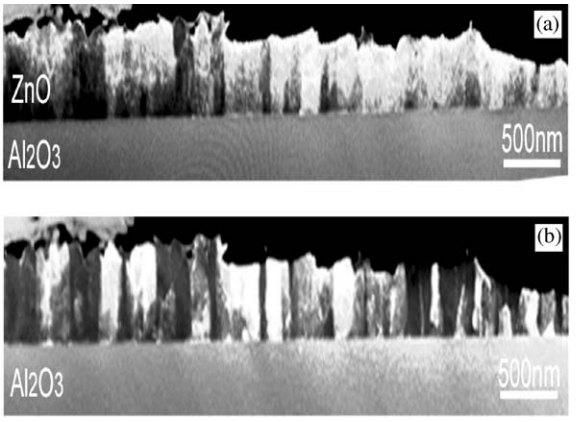

Fig. 1. XTEM micrographs (sample A without Ga) under weak-beam diffraction condition with vector $g = [0\,0\,0\,2]$ (a) and $[1\bar{1}\,0\,0]$ (b).

diffraction conditions with vector $g = [0\,0\,0\,2]$ and $[1\bar{1}00]$, respectively. It can be seen that defects with very high density (about $3 \times 10^{10}\,\mathrm{cm}^{-2}$) are obviously delineated in both images and the film shows an explicit feature of column domains. Although it is difficult to distinguish which particular dislocation these defects are, we can clearly find that the defects almost penetrate through the whole film through the sharp black/white contrast in the images which indicates the ZnO film has a poor quality. The result is consistent with the XRD measurement discussed later.

Figs. 2(a) and (b) show the cross-sectional TEM (XTEM) images of a ZnO/Ga/sapphire film (sample B) under weak-beam diffraction conditions with vector $g = [0\,0\,0\,2]$ and $[1\bar{1}\,0\,0]$, respectively. We can clearly see that defects with high density are confined at the interface and intensive interaction of the defects results in a rapid decrease of the dislocation density in the upper region of the ZnO film. The dominant defects in the film are TDs resulting from the misfit strain introduced by the lattice mismatch between the epilayer and substrate. According to the nature of the defects, there are three different regions, as delineated by Fig. 2: (I) the interface region with a thickness $h = 75\,\mathrm{nm}$.The white contrast indicates that very high-density misfit dislocations form in this region; (II) the middle region of $75\,\mathrm{nm} < h < 255\,\mathrm{nm}$, where the defects decrease and interactions between screw-component dislocations are reduced, partly associated with the formation of basal plane dislocations (BPD); (III) the upper region from $h = 255\,\mathrm{nm}$ to the film free surface. In this region, the TDs are decreased significantly and very little interaction is observed. The total threading dislocation density in this region is approximately $8 \times 10^8\,\mathrm{cm}^{-2}$, calculated according to $D = n/lh$ [13], where n, l, h is the number of the dislocations, foil length and thickness in cross-sectional specimen, respectively. Comparing Fig. 2(a) to Fig. 2(b), we can clearly see that in the regions (I) and (II) most dislocations are observed in both the $g = 1\bar{1}\,0\,0$ and $0\,0\,0\,2$ images. This indicates that the major defects are mixed-type dislocations in the initial and buffer layer stage, since they have a character of Burgers vector $b = \frac{1}{3}[1\,1\,\bar{2}\,3]$ and are visible in two different diffraction conditions [13]. Moreover, we can also observe that dislocations interact strongly within these regions and some loops associated with mixed- and screw-type dislocations are formed. Thus, most TDs are confined within these two regions due to the dislocation interaction leading to a dramatic reduction of TDs in the upper region III of the film, as observed in Fig. 2. Within the limit of imaging statistics, we also found that there are approximately 60% edge-type ($b = \frac{1}{3}[1\,1\,\bar{2}\,0]$) and 40% mixed-type dislocations. No pure screw dislocation ($b = \frac{1}{2}[0\,0\,0\,2]$) is present in region (III). The remarkable reduction of screw-component dislocations from regions (I) and (II) to region (III) is well consistent with the XRD measurements discussed below. In other words, by using an ultrathin gallium as a wetting layer on sapphire substrate, the defects of the ZnO film are prominently decreased.

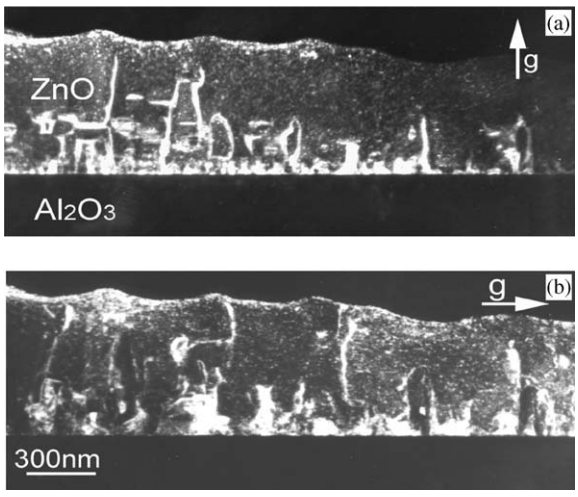

Fig. 2. XTEM micrographs (sample B with Ga) under weak-beam diffraction condition with vector $g = [0\,0\,0\,2]$ (a) and $[1\bar{1}\,0\,0]$ (b).

Fig. 3 shows the XRD ω-rocking curves of ZnO $(0\,0\,0\,2)$ and ZnO $(1\,0\,\bar{1}\,2)$ for both samples A and B. Basically, the rocking curve of symmetric plane is broadened mainly due to the screw or mixed-type dislocations in a mosaic structure, similar to the GaN or ZnO epilayers on $(0\,0\,0\,1)$ sapphire substrate [7,14]. Pure edge dislocations have little contribution to the broadening of the $(0\,0\,0\,2)$

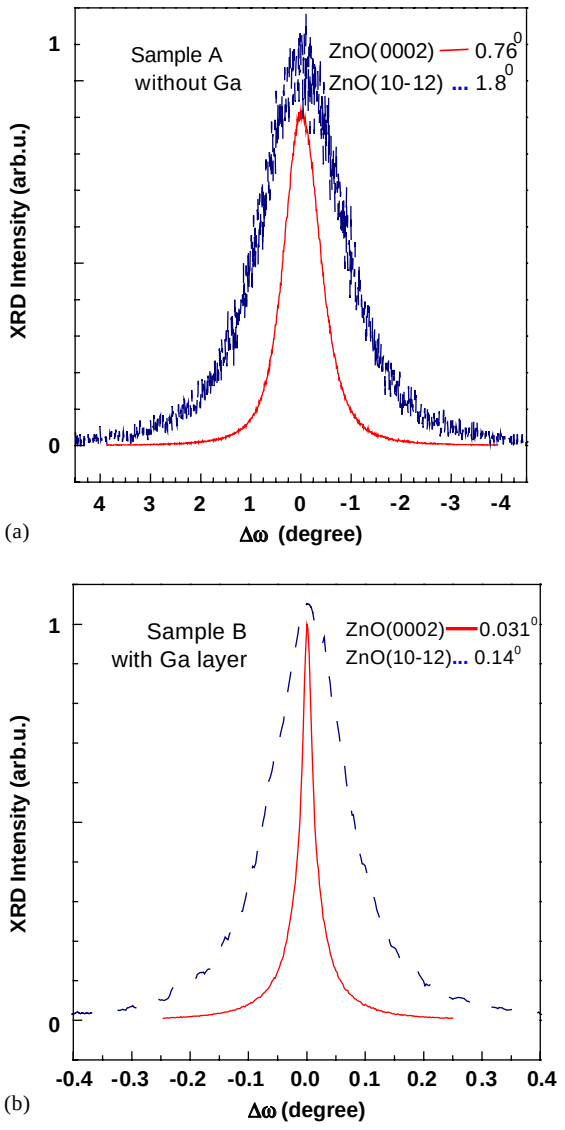

Fig. 3. XRD ω–rocking curve of the ZnO (0 0 0 2) and ZnO (10 $\bar{1}$2) diffraction peaks, (a) sample A, (b) sample B. The line shape of ZnO (0 0 0 2) for sample B consists of a very broad peak overlapping a sharp central peak with the FWHM around 0.031 °.

ω-rocking curve, whereas the rocking curve broadening of asymmetric plane, such as ZnO(1 0 $\bar{1}$ 2), is attributed to all three kinds of TDs. The full width at half-maximum (FWHM) values of both ZnO(0 0 0 2) and ZnO(1 0 $\bar{1}$ 2) diffraction peaks for sample A are very big (Fig. 3(a)), illustrating huge densities of both pure-edge TDs and TDs with screw component. For sample B, on the other hand, ZnO(0 0 0 2) diffraction peak is very narrow (Fig. 3(b)), its FWHM is as small as 0.031 °, indicating a very low density of screw and mixed dislocations. The sharp peak is accompanied by a long tail, and is most likely related to a region with a high density of screw-component dislocations near the interface, which has been confirmed by the above TEM observations. It is interesting to note that, in Fig. 2, the line direction of the mixed-type dislocations has either an inclined angle of approximately 11 ° or negative 11 ° to the surface normal. This value is close to the calculated value (15.6 °) by Mathis et al. [15]. It is well known that these inclined mixed-type dislocations will interact with other dislocations when they propagate upward, the interaction will lead to a great reduction of threading dislocation density in the upper region. Therefore, with the ultrathin Ga wetting layer, most dislocations are confined within the interface and initial layer. This is compared to the report by Vigué et al. [6], Hong et al. [7] and our ZnO film without Ga wetting layer (sample A), where most TDs formed at the interface penetrate through the entire ZnO films grown on (0 0 0 1) sapphire or (0 0 0 1) GaN without any wetting layer.

From the above XRD analysis and TEM results, we can obviously see that, by using an ultrathin Ga wetting layer, the defects of the ZnO film were prominently reduced and the quality of the film was well improved. Based on our TEM observations, we propose a model to explain the remarkable reduction of screw-component dislocations in sample B. It has been reported that impurity doping to a certain extent, in GaN film could decrease the dislocation density by forming pinnings associated with BPD that promoted the dislocation interactions compared to undoped one, such as Si doping in GaN [16–18]. However, an unsuitable doping would lead to high density of basal plane stacking faults [19]. Here, we suggest that a small quantity of Ga diffused from the film/substrate interface acts as an impurity dopant and plays a key role in the formation and reduction of screw-component dislocations in the ZnO film. An oxygen-terminated surface of sapphire (0 0 0 1) substrate is expected to form after oxygen plasma

irradiation. However, this surface is not stable due to the oxygen desorption in vacuum, and oxygen and aluminum-terminated regions coexist. On this surface, after Ga deposition, Ga atoms can form two kinds of bonds, the strong one on the oxygen-terminated region, and the weak one on the aluminum-terminated region. The Ga atoms deposited on the oxygen terminated regions will serve as template for ZnO, whereas the Ga atoms on aluminum terminated regions will diffuse into the ZnO film in terms of the weak bonding between Ga and Al. When the first ZnO layer nucleates on the Ga- and Al-terminated regions, a height difference will result in the ZnO islands. The height difference will cause the formation of screw-component dislocations when coalescence of the 2D ZnO islands nucleated on different regions occurs. During the coalescence, some oxygen dangling bonds are available along the surface step edges and the diffusing Ga atoms will be captured, forming BPD. Since the step edges are associated with screw, rather than edge dislocations, the Ga incorporation at steps inhibits the step growth of ZnO, which will lead to the screw-component dislocations bending over the basal plane [16]. However, two vicinal screw dislocations with opposite Burgers vector can be paired together to form a dislocation loop [2,16,20], as shown in Fig. 4. For a pure screw dislocation, due to formation of the Ga–O bonds at the step edge, it can be bent and will be paired to form a dislocation loop if the other with converse Burgers vector is available in the vicinal regions (as the inner loop shown in Fig. 4(a)). Or, they may interact to form another threading dislocation if the other dislocation is not pure screw-type (see the outer loop with a protruding dislocation shown in Fig. 4(a)). In the case no dislocation is available in the vicinal region, it will bend back into the origin direction, i.e. the growth direction, leaving behind a kink (the left one in Fig. 4(b)). As for mixed-type dislocations, the screw-component ones did the similar way as discussed above, and we even found such dislocations that contain several kinks associated with BPD, as shown in the right part of Fig. 4(b).

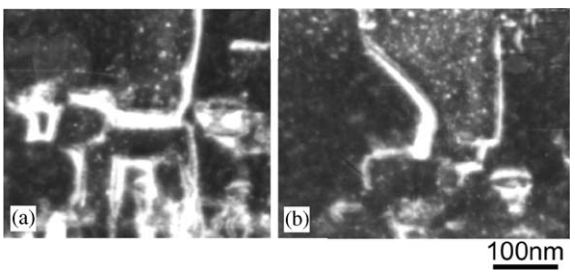

Fig. 4. Micrographs of dislocation loops (a) and dislocations containing kinks (b) formed by the pinning of Ga–O associated with BPD, taken with $g = 0002$.

In addition, inversion domains [8,13,21], which often exist in epitaxial ZnO and GaN films are not observed, and our ZnO films has a single [0 0 0 1] polarity (i.e. Zn polarity) [11]. This probably indicates that the Ga wetting layer is relatively well covered over the sapphire substrate. As discussed above, even if oxygen desorbs, the deposited Ga atoms diffuse to form two kinds of nucleation sites for the first ZnO layer: Ga or Al, leading to the stacking sequence of Ga (Al)–O–Zn–, and thus a sole Zn polarity.

4. Conclusions

In summary, we have characterized the defect structures of the ZnO films grown using an ultrathin Ga wetting layer by TEM and XRD compared to the ZnO film without Ga wetting layer. It was found that by applying an ultrathin Ga as a wetting layer on the sapphire substrate, the defects of the ZnO film were prominently reduced and a high-quality film was formed. Within this ZnO film, The remarkable reduction of screw-component dislocations leads to a total dislocation density of as low as $8 \times 10^8\,cm^{-2}$ in the upper part of the epitaxial film. And almost no pure screw dislocations were observed, neither were inversion domains. It was found that Ga has played a key role in defect reduction and inversion domain suppression.

Acknowledgements

This work was supported by National Science Foundation of China under Contract Nos.

60376004, 10174089 and 60021403, and Ministry of Science and Technology of China under Contract No. 2002CB613500.

References

[1] T. Mitate, Y. Sonoda, N. Kuwano, Phys. Stat. Sol. A 192 (2002) 383.
[2] S.-H. Lim, D. Shindo, H.-B. Kang, K. Nakamura, J. Vac. Sci. Technol. B 19 (1999) 506.
[3] S.-H. Lim, J. Washburm, Z. Liliental-Weber, D. Shindo, J. Vac. Sci. Technol. A 19 (2001) 2601.
[4] E.K. Sanchez, J.Q. Liu, M. De Graef, M. Skowronski, W.M. Vetter, M. Dudley, J. Appl. Phys. 91 (2002) 1143.
[5] T. Nakamura, Y. Yamada, T. Kusumori, H. Minoura, H. Muto, Thin Solid Films 411 (2002) 60.
[6] F. Vigué, P. Vennéguès, S. Vézian, M. Laügt, J.-P. Faurie, Appl. Phys. Lett. 79 (2001) 194.
[7] S.-K. Hong, H.-J. Ko, Y. Chen, T. Yao, J. Crystal Growth 209 (2000) 537.
[8] J. Narayan, K. Dovidenko, A.K. Sharma, S. Oktyabrsky, J. Appl. Phys. 84 (1998) 2597.
[9] S. Hong, T. Hanada, H. Ko, Y. Chen, T. Yao, D. Imai, K. Araki, M. Shinohara, K. Saitoh, M. Terauchi, Phys. Rev. B 65 (2002) 115331.
[10] Y. Chen, S.-H. Hong, H.-J. Ko, V. Kirshner, H. Wenisch, T. Yao, K. Inaba, Y. Segawa, Appl. Phys. Lett. 78 (2001) 3352.
[11] Y. Wang, Q.Y. Xu, X.L. Du, Z.X. Mei, Z.Q. Zeng, Q.K. Xue, Z. Zhang, Phys. Lett. A 320 (2004) 322.
[12] X.L. Du, M. Murakami, H. Iwaki, Y. Ishitani, A. Yoshikawa, Jpn. J. Appl. Phys. 41 (2002) L1043.
[13] X.H. Wu, L.M. Brown, D. Kapolnek, S. Keller, B. Keller, S.P. DenBaars, J.S. Speck, J. Appl. Phys. 80 (1996) 3228.
[14] B. Heying, X.H. Wu, S. Keller, Y. Li, D. Kapolnek, B.P. Keller, S.P. DenBaars, J.S. Speck, Appl. Phys. Lett. 68 (1996) 643.
[15] S.K. Mathis, A.E. Romanov, L.F. Chen, G.E. Beltz, W. Pompe, J.S. Speck, J. Crystal Growth 231 (2001) 371.
[16] O. Contreras, F.A. Ponce, J. Christen, A. Dadgar, A. Krost, Appl. Phys. Lett. 81 (2002) 4712.
[17] T. Paskova, E. Valcheva, J. Birch, S. Tungasmita, P.O.Å. Persson, R. Beccard, M. Heuken, B. Monemar, J. Appl. Phys. 88 (2000) 5729.
[18] S.l. Molina, A.M. Sánchez, F.J. Pacheco, R. García, M.A. Sánchez-García, F.J. Sánchez, E. Calleja, Appl. Phys. Lett. 74 (1999) 3362.
[19] Hyung Koun Cho, Jeong Yong Lee, Seong Ran Jeon, Gye Mo Yang, Appl. Phys. Lett. 79 (2001) 3788.
[20] J.L. Rouviere, M. Arlery, B. Daudin, G. Feuillet, O. Briot, Mater. Sci. Eng. B 50 (1997) 61.
[21] H. Zhou, T. Rupp, F. Phillipp, G. Henn, M. Gross, A. Rühm, H. Schröder, J. Appl. Lett. 93 (2003) 1933.